Title
Threshold vibrational excitation of CO{sub 2} by slow electrons

Authors
Vanroose, Wim
Zhang, Zhiyong
McCurdy, C.W.
et al.

Publication Date
2003-07-08

Threshold vibrational excitation of CO_2 by slow electrons

Wim Vanroose, Zhiyong Zhang, C. W. McCurdy, and T. N. Rescigno
Computing Sciences, Lawrence Berkeley National Laboratory, One Cyclotron Road, Berkeley, CA 94720
(Dated: November 26, 2003)

Threshold structures, reminiscent of those seen in the polar hydrogen halides, have recently been observed in the cross sections for electron impact excitation of certain vibrational levels of the non-polar CO_2 molecule. These structures occur at energies outside the range where shape resonances dominate the dynamics. We propose a virtual state model that describes the multi-dimensional nuclear dynamics during the collision and explains quantitatively the selectivity observed in the excitation of the Fermi dyad, as well as the pattern of threshold peaks and oscillations seen in the upper levels of the higher polyads.

PACS numbers: 34.80.Gs

For certain molecules, the cross sections for electrons exciting vibrations at very low energies can deviate markedly from the behavior predicted by simple threshold laws, displaying pronounced structures within a few tenths of an electron volt (eV) of threshold. Rohr and Linder [1] first observed such structures some twenty-five years ago in the hydrogen halides (HF, HCl and HBr) and initiated a period of intense experimental and theoretical activity that has continued to the present [2, 3]. Of the various factors that come into play in these systems, an essential component seems to be the fact that, for very low-energy collisions, the target provides the electron with a potential well that is on the verge of binding an extra electron. Small displacements of the nuclei away from equilibrium can cause the composite electron+target system to shift from being a bound state to an unbound "virtual state" [4], leading to strong coupling between electronic and nuclear motion. Much of the work in this area has been focused on the hydrogen halides - systems with only one nuclear degree of freedom. Recent experiments by Allan [5, 6] have revealed interesting polyatomic effects in the threshold vibrational excitation cross sections for *non-polar* targets like CO_2 and CS_2.

The principal features of e-CO_2 scattering have been known for decades. Peculiarities in the threshold vibrational excitation cross sections were first observed in 1985 [7]; the suggestion of a virtual state being responsible for the low-energy enhancement of the cross sections came even earlier [8]. In these early studies, the target vibrational levels were described in terms of uncoupled normal modes. But an accidental degeneracy between one quantum of symmetric stretch and two quanta of bend invalidates this simple picture since it leads to a strong mixing of the zeroth order levels (or so-called polyads) known as "Fermi resonance" [9]. With a decisive improvement in energy resolution, Allan has been able to measure excitation cross sections for individual components of the polyads in CO_2; he makes the striking observation that there is not only structure, but also selectivity in these excitation cross sections. For the Fermi dyad, Allan's [5] measurements reveal that one component displays a pronounced threshold peak while the other level has a vanishingly small cross section at low energy. Allan also observed a pattern of threshold peaks and oscillatory structure in the upper levels of the higher polyads. Both observations have yet to be explained. Our purpose here is to describe a theoretical model that provides a quantitatively accurate description of this data.

The principal assumption of our treatment is that, for very small electron energies, the excitation cross sections are entirely determined by the Born-Oppenheimer potential surface of the molecular anion and its analytic continuation to geometries where it is unbound. For geometries where the anion is electronically bound relative to the neutral, we can use electronic structure methods to compute the relevant energy surfaces. We have restricted our investigation to C_{2v} geometries where both CO bond distances are equal and the O-C-O angle is allowed to vary, i.e. we ignore asymmetric stretch motion.

Neutral CO_2 is linear at equilibrium (with a CO bond distance of 2.2 bohr) while CO_2^- is correspondingly unbound at the same geometry. If we stretch the CO bonds, keeping the atoms collinear, the anion becomes bound for CO distances greater than $\sim$2.55 bohr [10], correlating with the CO + O^- dissociation limit. It is easy to see that there must be two quasi-degenerate anion states at these stretched, linear geometries. O^- has the configuration ^{2}P and CO is a closed-shell. There are thus two anion states, of $^2\Pi$ and $^2\Sigma$ symmetry, corresponding to configurations where the O^- p-shell vacancy is aligned either perpendicular or parallel to the CO axis, respectively. As the CO bonds are compressed, these states move apart and eventually become unbound: the $^2\Pi$ state moves up into the continuum relative to CO_2 and becomes the 3.8 eV shape resonance, while the $^2\Sigma$ state becomes a virtual state.

It is now established that the $^2\Pi_u$ CO_2^- shape resonance, near 3.8eV, is not involved in the threshold regions. It is too high in energy and, as recently shown by McCurdy *et al* [11], only the features in cross sections above 1.5 eV can accuratly be predicted through multi-dimensional "boomerang" dynamics on the $^2A_1$ and $^2B_1$

components of the $^2\Pi_u$ shape resonance that are coupled through Renner-Teller effects. But below those energies, the boomerang model does not accurately describe the excitation cross sections. It is the virtual state, defined by analytic continuation of the bound CO_2^- $^2\Sigma$ state, that determines the threshold nuclear excitation dynamics.

If we bend the CO_2 molecule, it acquires a dipole moment which increases its electron affinity. In her 1998 study, Morgan [12] showed how the virtual state of CO_2^- evolved into a $^2A_1$ bound anion as the molecule was bent, with the CO bond distances fixed. As the OCO angle changes from 180^o to 145^o, the virtual state, which starts on the negative imaginary axis of the complex momentum (K) plane, moves off the axis and approaches the origin on a curved trajectory that has a kink at K=0, where the anion becomes bound. More recently, Sommerfeld [13] reported another cut through the CO_2^- surface in C_{2v} symmetry, along a vector connecting the minimum on the anion surface (at a CO distance of 2.3 bohr and O-C-O angle of 138^o) with the equilibrium geometry of the neutral. He found that the CO_2^- curve exhibits a barrier between 150^o and 155^o just before it crosses the neutral curve. Sommerfeld did not attempt to characterize the anion curve after it crossed the neutral curve.

We need a strategy to construct a complete $^2A_1$ anion surface in C_{2v} geometry. So calulations were carried out on the neutral molecule using the coupled-cluster method to determine the ground state potential surface and the dipole moment function for a range of CO bond distances and O-C-O angles in C_{2v} geometry. We then carried out coupled-cluster calculations for the $^2A_1$ anion surface at corresponding geometries where it is electronically bound. From these calculations, we can characterize the "seam", as a function of O-C-O angle (Θ) and CO bond distance (R), where the neutral and anion surfaces intersect. We denote the values of R and Θ along the seam as (R_o, Θ_o). To analytically continue the anion surface beyond this seam, we begin by writing $V_{ion}(R,\Theta) = V_{neutral}(R,\Theta) + \frac{1}{2}K^2(R,\Theta)$. We can think of $K(R,\Theta)$ as the (complex) momentum of the electron in the negative ion. Where the ion is bound, K is a positive imaginary number. It moves into the lower half-plane when the anion is unbound. The topology of the complex surface, $K(R,\Theta)$, near $K = 0$ is determined by the behavior of the electron-molecule interaction at large distances, i.e. by the dipole moment of the neutral, which depends on R and Θ. Where the dipole vanishes, quadrapole and polarization interactions could slightly modify the behavior of K, but this would only effect the complex portion of the anion surface at linear geometry.

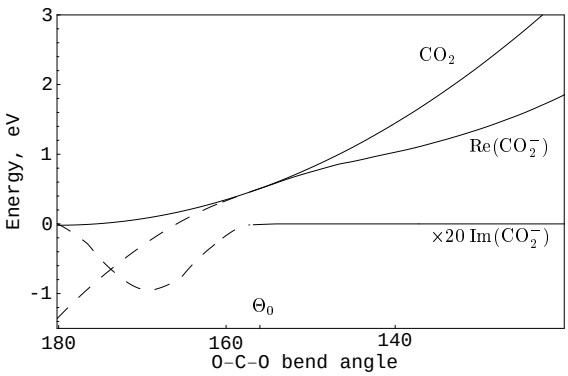

FIG. 1: Cuts through the potential surfaces of CO_2 and CO_2^- where the O-C-O angle Θ, in degrees, is varied and the C-O bond distance is fixed at 2.2 bohr. In the crossing region, around Θ_0, the difference between the curves follows a threshold law predicted by the dipole moment of CO_2. This law allows us to analytically continue the CO_2^- potential into configurations where it is unbound, denoted by dashed curves, and construct a complete surface for the CO_2^- virtual state.

The binding properties of a fixed dipole potential are well known and have been studied by a number of authors. We follow the treatment of Lévy-Leblond [14]. The Schrödinger equation for an electron in a dipole field is separable in polar coordinates. For small dipole moments, which is the case we have here, only the lowest (nodeless) angular mode gives rise to an attractive centrifugal potential. The effective angular momentum, l, of the electron in this mode is a negative real number between $-\frac{1}{2}$ and zero which depends on the value of the dipole moment, D. The relationship between l and D was given by Lévy-Leblond as a power series, $l(l+1) = 2D(R,\Theta)^2/3 + \ldots$. To determine K, we need to examine the Jost function, $\mathcal{F}_l(K)$, for this dipole problem and determine the values of K for which the Jost function vanishes. This problem is discussed by Newton [4].

Along the seam (R_o, Θ_o), K is zero. Following Newton, we expand the Jost function around K=0 as $\mathcal{F}_l(K) = a_0 + a_2K^2 + \ldots + ib_1K^{2l+1} + \ldots$. The a and b coefficients, which depend on nuclear geometry, are also expanded about (R_o, Θ_o). Keeping only terms through first order, we can characterize K in the vicinity of the crossing as

$$K(R,\Theta) = i(\alpha(R-R_0) + \beta(\Theta-\Theta_0))^{1/(2l(R,\Theta)+1)} \quad (1)$$

where α and β are constants. $l(R,\Theta)$ is related to $D(R,\Theta)$, by Lévy-Leblond's power series. The only unknowns are the constants α and β and these are chosen so to give a smooth connection between the inner and outer portions of the anion surface. We have thus used the analytic properties of the dipole potential to connect the complex part of the anion surface to the real part that was determined *ab initio*. Figure 1 shows a cut through our calculated neutral and anion surfaces at a fixed CO bond distance. Since the molecule is slightly bent in the crossing region, and therefore has a weak dipole moment, the exponent in Eq. (1) is non-integer and the CO_2^- surface becomes complex as soon as $(\Theta - \Theta_0)$ switches sign. These independently computed potential surfaces are consistent with both Morgan's [12] and Sommerfeld's [13] calculations.

Having constructed an anion potential surface, we need a dynamical equation to describe the nuclear motion and to evaluate the vibrational excitation cross sections. The zero-range potential model of Gauyacq and Herzenberg [15] is our starting point for developing a nuclear wave equation. The basic assumption of the model is that, at very low energies, the wave function that describes the scattered electron is independent of energy inside some radius r_o. Inside this radius, the potential is strong and the electron follows the nuclei adiabatically. The logarithmic derivative of the wave function , $f(R,\Theta) = \frac{\partial\psi(r\,;R,\Theta)}{\partial r}/\psi(r\,;R,\Theta)$, at r $=r_o$ is introduced to avoid calculations in the inner region. The fact that there is a zero in the Jost function close to the origin means that the wave function inside r_o can be equated with a purely outgoing wave (Siegert state) of the form $\psi(r\,;R,\Theta) \sim \exp\left(iK(R,\Theta)r - l(R,\Theta)\pi/2\right)$.[15] It follows that $f(R,\Theta) = iK(R,\Theta)$.

Asymptotically, where the scattered electron is outside the molecule, we can express its wave function, using S-matrix boundary conditions, as:

$$\psi(r\,;R,\Theta) \underset{r\to\infty}{=} h_l^-(k_o r)\phi_0(R,\Theta) + \sum_n A_n h_l^+(k_n r)\phi_n(R,\Theta) \tag{2}$$

where the $\phi_n(R,\Theta)$'s, with energies E_n, are the vibrational states of neutral CO_2 and $h^{+(-)}$ is an outgoing(incoming) Hankel function. The channel momenta, k_n must satisfy $k_n = \sqrt{2(E-E_n)}$ to ensure energy conservation. For energetically open channels, the A_n are related to vibrational excitation cross sections by

$$\sigma_{0n} = \frac{\pi}{k_0^2}\frac{k_n}{k_0}|A_n|^2, \quad \text{if} \quad E > E_n \tag{3}$$

The next step is to equate the log-derivative of ψ, evaluated using Eq. (2 at r_o, with $iK(R,\Theta)$. The matching condition can be converted to a system of linear equations by using an expansion in target vibrational states and integrating over their internal coordinates. If one further assumes that r_o can be chosen large enough so that the Hankel functions can be replaced by their asymptotic forms, then it is easily shown that the matching equations become independent of r_o.[16] Gauyacq and Herzenberg [15] used this line of reasoning some time ago, treating K as an empirical parameter adjusted it to fit experiment, to model the threshold vibrational structures seen in e^-+HCl scattering. Their procedure can diverge at certain collision energies unless continuum target states are included in the expansion and, in any case, is not practical for polyatomic molecules. The matching condition, as we have recently shown [17], can be reorganized into an equivalent differential equation. Moreover, our analytic continuation procedure for constructing the complete anion surface obviates the need for treating $K(R,\Theta)$ empirically. The key to the derivation, which is detailed in ref. [17], is to begin with the matching condition and to use the operator identity $k_n\phi_n = \sqrt{2(E-H_{neutral})}\phi_n$. There we show that by defining $\sum_n A_n e^{i(k_n+k_0)r_0}\phi_n = \left(K + \sqrt{2(E-H_{neutral})}\right)\Psi$, one can derive the equation:

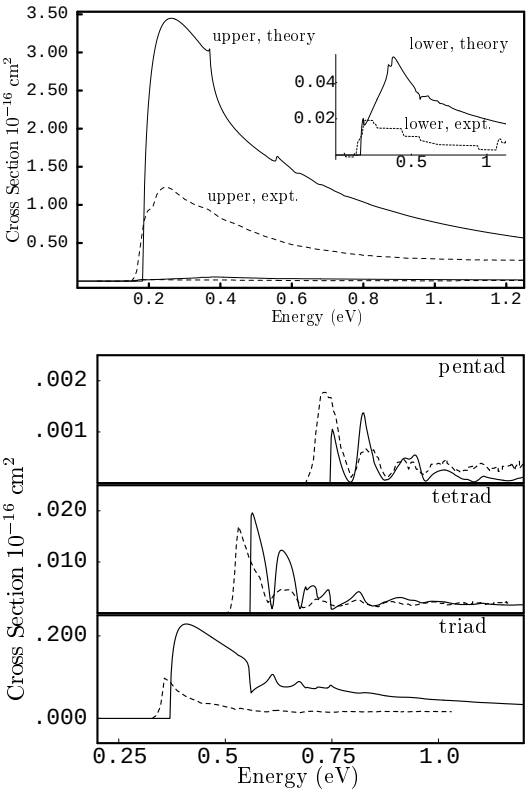

FIG. 2: Excitation cross sections for the Fermi polyads in CO_2. Solid lines: theory; dashed lines: experiment (ref. [5, 6]). Top panel: dyad; bottom panel: triad, tetrad and pentad.

$$\left(2(E-H_{ion}) + \left[\sqrt{2(E-H_{neutral})}, K(R,\Theta)\right]\right)\Psi = \left(K(R,\Theta) + k_0\right)\phi_0. \tag{4}$$

Since the variation of K with geometry is significant, especially in the vicinity of the crossing seam between neutral molecule and anion, the commutator in Eq. (4) is non-negligible and carries significant non-local effects.

We solved Eq. (4) in normal coordinates using a two-dimensional discrete variable representation (DVR) of the nuclear wave equation, as outlined in ref. [11]. The operator $\sqrt{2(E-H_{neutral})}$ was represented in terms of the matrix eigenvalues and eigenvectors of $H_{neutral}$ in the finite DVR basis [17]. The excitation amplitudes A_n are obtained as $A_n = \langle\phi_n|K + k_n|\Psi\rangle$ and the cross sections are evaluated using Eq. (3). We show the resulting vibrational excitation cross sections in Figure 2.

The selectivity seen in the excitation cross sections for the two components of the dyad is the result of two effects. First, there is the complex part of the $^2A_1$ surface that forces Ψ to decay in regions where the magnitude of

the imaginary part of the energy is large. As we see in Figure 3, the complex part of the CO_2^- surface is large for small C-O bond lengths and slightly bent geometries. The lower member of the dyad, shown in the bottom panel of the figure, has a significant probability in this shaded region, while the upper member, plotted in the top panel, has a smaller overlap. This results in a larger cross section for the upper member. More important in determining the selectivity, however, is the commutator in Eq. (4). As discussed earlier, that term is most important in the crossing region. The upper member of the dyad comes closer to the crossing region and, therefore, has a much bigger interaction with the electronic motion.

The same effects come into play in the cross sections for excitation to the higher polyads. In the triad, for example, only the upper member has significant probability close to the crossing seam and, consequently, its cross section is greatly enhanced versus the other vibrations of the triad. As we increase the electron energy and excite states higher up in the CO_2 vibrational spectrum, the temporary negative ion probes larger portions of the $^2A_1$ surface, including regions where the anion state is bound relative to the neutral. Almost all the members of the polyads now cross the seam and the selectivity between them is not as pronounced. However, nuclear motion is so strongly coupled to the electronic motion at the seam, that the dynamics near the seam is sensitive to the opening of new vibrational channels. This effect appears in the theoretical and experimental cross sections of the top members of the triad, tetrad and pentad shown in Figure 2. The opening of a new channel eats a hole in the cross sections of vibrational channels that were already open.

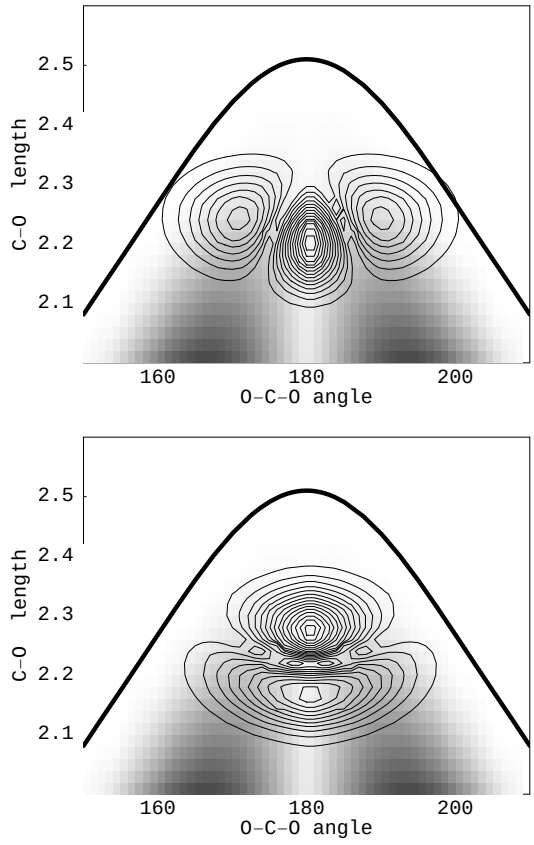

FIG. 3: Contour plots of the wave functions for the two components of the Fermi dyad in O-C-O angle, in degrees, and C-O bond distance, in bohr. The thick line marks the seam where the anion and neutral surfaces cross. The imaginary part of the anion surface is zero above the seam and increases proportionately in regions indicated by the shading. Top panel: upper member of dyad; bottom panel: lower member of dyad.

In summary, we have shown how a simple threshold law describes the $^2A_1$ electronic surface of the virtual state. Only two dimensional dynamics that include non-Born-Oppenheimer effects on this surface can predict the selectivity and the oscillating structures seen in the experiment. Slow electrons interact strongly with vibrational states that probe configurations where the CO_2 and CO_2^- potential curves cross.

The authors acknowledge helpful discussions with H.-D Meyer and T. Sommerfeld. This work was performed under the auspices of the US Department of Energy by the University of California Lawrence Berkeley National Laboratory and supported by the DOE Office of Basic Energy Science, Division of Chemical Sciences.

[1] K. Rohr and F. Linder, J. Phys. B **9**, 2521 (1976).
[2] M. Cizek, J. Horacek, M. Allan, I. I. Fabrikant, and W.Domcke, J. Phys. B **36**, 2837 (2003).
[3] M. Cizek, J. Horacek, A.-C. Sergenton, D. B. Popovic, M. Allan, W.Domcke, T. Leinenger, and F. X. Gadea, Phys. Rev. A **63**, 062710 (2001).
[4] R. G. Newton, *Scattering Theory of Particles and Waves* (Springer-Verlag, New York, 1982), 2nd ed.
[5] M. Allan, J. Phys. B **35**, L387 (2002).
[6] M. Allan, Phys. Rev. Lett. **87**, 033201 (2001).
[7] K.-H. Kochem and et al., J. Phys. B **18**, 4455 (1985).
[8] M. A. Morrison, Phys. Rev. A **25**, 1445 (1982).
[9] G. Herzberg, *Molecular Spectra and Molecular Structure II. Infrared and Raman Spectra of Polyatomic Molecules* (Van Nostrand Reinhold, 1945).
[10] T. N. Rescigno, W. A. Isaacs, A. E. Orel, H.-D. Meyer, and C. W. McCurdy, Phys. Rev. A **65**, 032716 (2002).
[11] C. W. McCurdy, W. A. Isaacs, H.-D. Meyer, and T. N. Rescigno, Phys. Rev. A **67**, 042708 (2003).
[12] L. A. Morgan, Phys. Rev. Lett. **80**, 1873 (1998).
[13] T. Sommerfeld, J. Phys. B **36**, L127 (2003).
[14] J.-M. Lévy-Leblond, Phys. Rev. A **153**, 1 (1967).
[15] J. P. Gauyacq and A. Herzenberg, Phys. Rev. A **25**, 2959 (1982).
[16] J.-P. Gauyacq, *Dynamics of Negative Ions* (World Scientific, Singapore, 1987).
[17] W. I. Vanroose, C. W. McCurdy, and T. N. Rescigno, Phys. Rev. A **68**, 052713 (2003).